JOURNAL OF GEOPHYSICAL RESEARCH: OCEANS, VOL. 118, 5312–5321, doi:10.1002/jgrc.20378, 2013

Tropical cyclones cause $CaCO_3$ undersaturation of coral reef seawater in a high-CO_2 world

Derek Manzello,[1,2] Ian Enochs,[1,2] Sylvia Musielewicz,[3] Renée Carlton,[1,2] and Dwight Gledhill[4]

Received 22 May 2013; revised 23 July 2013; accepted 26 August 2013; published 15 October 2013.

[1] Ocean acidification is the global decline in seawater pH and calcium carbonate ($CaCO_3$) saturation state (Ω) due to the uptake of anthropogenic CO_2 by the world's oceans. Acidification impairs $CaCO_3$ shell and skeleton construction by marine organisms. Coral reefs are particularly vulnerable, as they are constructed by the $CaCO_3$ skeletons of corals and other calcifiers. We understand relatively little about how coral reefs will respond to ocean acidification in combination with other disturbances, such as tropical cyclones. Seawater carbonate chemistry data collected from two reefs in the Florida Keys before, during, and after Tropical Storm Isaac provide the most thorough data to-date on how tropical cyclones affect the seawater CO_2 system of coral reefs. Tropical Storm Isaac caused both an immediate and prolonged decline in seawater pH. Aragonite saturation state was depressed by 1.0 for a full week after the storm impact. Based on current "business-as-usual" CO_2 emissions scenarios, we show that tropical cyclones with high rainfall and runoff can cause periods of undersaturation ($\Omega < 1.0$) for high-Mg calcite and aragonite mineral phases at acidification levels before the end of this century. Week-long periods of undersaturation occur for 18 mol % high-Mg calcite after storms by the end of the century. In a high-CO_2 world, $CaCO_3$ undersaturation of coral reef seawater will occur as a result of even modest tropical cyclones. The expected increase in the strength, frequency, and rainfall of the most severe tropical cyclones with climate change in combination with ocean acidification will negatively impact the structural persistence of coral reefs.

Citation: Manzello, D., I. Enochs, S. Musielewicz, R. Carlton, and D. Gledhill (2013), Tropical cyclones cause $CaCO_3$ undersaturation of coral reef seawater in a high-CO_2 world, *J. Geophys. Res. Oceans*, *118*, 5312–5321, doi:10.1002/jgrc.20378.

1. Introduction

[2] Anthropogenic climate change is a leading threat to the future persistence of coral reefs [*Hoegh-Guldberg et al*., 2007]. The consequences of warming to reef-building corals, the building blocks of coral reefs, are particularly dire [*Frieler et al*., 2013]. The effects of ocean acidification have more recently begun to be investigated [*Kleypas et al*., 1999]. Lab and field-based studies have shown that acidification causes declines in coral calcification and increases biologically mediated reef dissolution [*Langdon et al*., 2000; *Yates and Halley*, 2006; *Silverman et al*., 2009; *Tribollet et al*., 2009]. Given that coral reef calcium carbonate ($CaCO_3$) production only slightly outpaces its physical, biological, and chemical breakdown, ocean acidification may work to accelerate the erosion of coral reef framework structures [*Hoegh-Guldberg et al*., 2007; *Manzello et al*., 2008]. Indeed, coral communities are less diverse and reef framework structures more susceptible to mechanical and biological erosion where ambient CO_2 levels are naturally elevated to levels expected with a doubling and tripling of atmospheric CO_2 [*Manzello*, 2009; *Fabricius et al*., 2011].

[3] Despite these dire predictions, we still understand relatively little about how coral reefs will respond to ocean acidification in combination with other disturbances, such as tropical cyclones. Tropical cyclones can cause mass mortality of corals and other reef associated organisms, as well as severe physical erosion to coral reef framework structures [e.g., *Goreau*, 1964; *Scoffin*, 1993]. Although it is not yet known if overall tropical cyclone frequency will change with climate change, the best existing models do indicate an increase in the frequency of the most intense storms and precipitation by 20% within 100 km of a storm's center [*Knutson, et al*., 2010; *Villarini and Vecchi*, 2012]. In situ environmental data during tropical cyclones are rare because instrumentation is often destroyed or lost

[1]Cooperative Institute for Marine and Atmospheric Studies, Rosenstiel School of Marine and Atmospheric Science, University of Miami, Miami, Florida, USA.
[2]Atlantic Oceanographic and Meteorological Laboratories, NOAA, Miami, Florida, USA.
[3]Joint Institute for the Study of the Atmosphere and Ocean, University of Washington—NOAA Pacific Marine Environmental Laboratory, Seattle, Washington, USA.
[4]Ocean Acidification Program, NOAA, Silver Spring, Maryland, USA.

Corresponding author: D. Manzello, Cooperative Institute for Marine and Atmospheric Studies, Rosenstiel School of Marine and Atmospheric Science, University of Miami, 4600 Rickenbacker Cswy., Miami, FL 33149, USA. (derek.manzello@noaa.gov)

2169-9275/13/10.1002/jgrc.20378

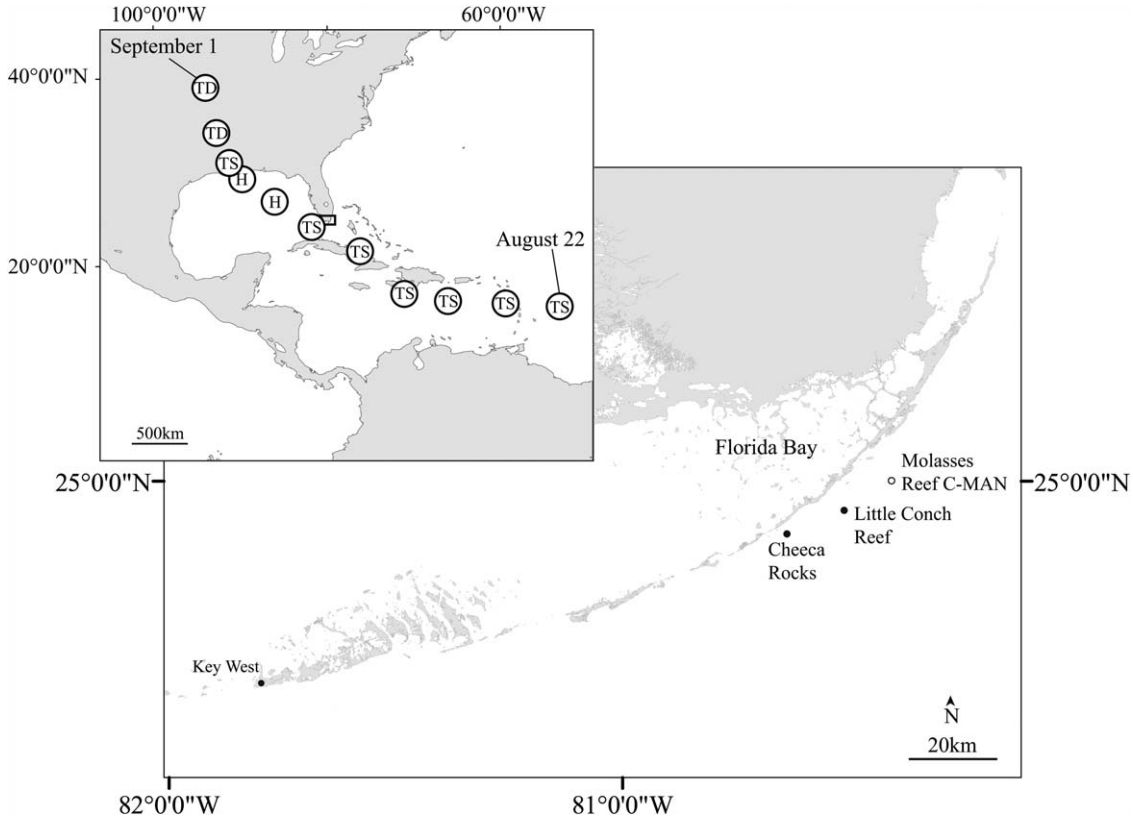

Figure 1. Location of study sites on Florida reef tract. Coral reef sites are dark circles, whereas open circle is location of SEAKEYS/C-MAN station. GPS coordinates are: Cheeca Rocks (24.8977N, 80.6182W), Little Conch Reef (24.9465N, 80.50207W), and Molasses Reef SEAKEYS/C-MAN (25.012N, 80.376W).

during storms. Only one prior study has documented the impact of a tropical cyclone on reef seawater carbonate chemistry. Intriguingly, these researchers measured their lowest pH and Ω value over 2 years of high-resolution monitoring as a result of a tropical storm [*Gray et al*., 2012]. In late August 2012, Tropical Storm (TS) Isaac passed approximately 142 km to the south of Cheeca Rocks in the Florida Keys (one of our study sites) at its closest point, providing the most thorough data to-date on how tropical cyclones impact seawater carbonate chemistry. Carbonate chemistry and environmental data collected at two reef sites on the Florida Reef Tract (FRT) before, during, and after the impact of TS Isaac in August and September 2012 are presented. Based on the response to TS Isaac, we model how tropical cyclones will impact reef seawater CO_2 when combined with seawater freshening from runoff, ocean acidification, and warming.

2. Methods

2.1. Carbonate Chemistry and Environmental Data

[4] Carbonate chemistry data were collected via a $MApCO_2$ (moored autonomous pCO_2) buoy and SeaFET pH sensor at Cheeca Rocks (depth = 5 m) on the FRT (Figure 1). An additional SeaFET pH sensor was deployed at Little Conch Reef (depth = 6 m) (Figure 1). Details on the $MApCO_2$ and SeaFET pH have been published [*Hofmann et al*., 2011; *Vandemark et al*., 2011]. In brief, the mole fraction of CO_2 (xCO_2) was measured with a nondispersive infrared gas analyzer on the $MApCO_2$ and the SeaFET pH data were on the total scale. The partial pressure of seawater CO_2 ($pCO_{2,sw}$) was calculated from the $xCO_{2,sw}$ buoy data with in situ sea temperature at 1 atmosphere. With pH and $pCO_{2,sw}$, we calculated the remaining carbonate parameters with the CO2SYS computer program [*Lewis and Wallace*, 1998] as previously described [e.g., *Manzello*, 2010]. Wind data were obtained from the Molasses Reef C-MAN station (available online: http://ecoforecast.coral.noaa.gov) and light intensity (photosynthetically active radiation, PAR) was measured at both sites using a LI-192SA LI-COR underwater quantum sensor at the same depths as the SeaFET pH sensors. The 5 days before the storm (16–21 August) were used as the prestorm baseline, whereas the poststorm period was 28 August to 4 September. Buoy data were not collected 23–28 August due to procedures to pre-empt possible storm damage, thus only pH data are available during the storm.

[5] Salinity data were not reported because the conductivity-temperature sensor on the MApCO2 data malfunctioned and was not working during the storm. Salinity data were collected on 22 August and the mean ± std error was 36.34 ± 0.037 for seven samples. A salinity value of 36.34 was used for all prestorm data (up to 23 August). Salinity data then were not collected until 4 September, beginning at 11:40 local time every minute. All the data (n = 740) had a mean salinity of 36.10. For the 7 days of data

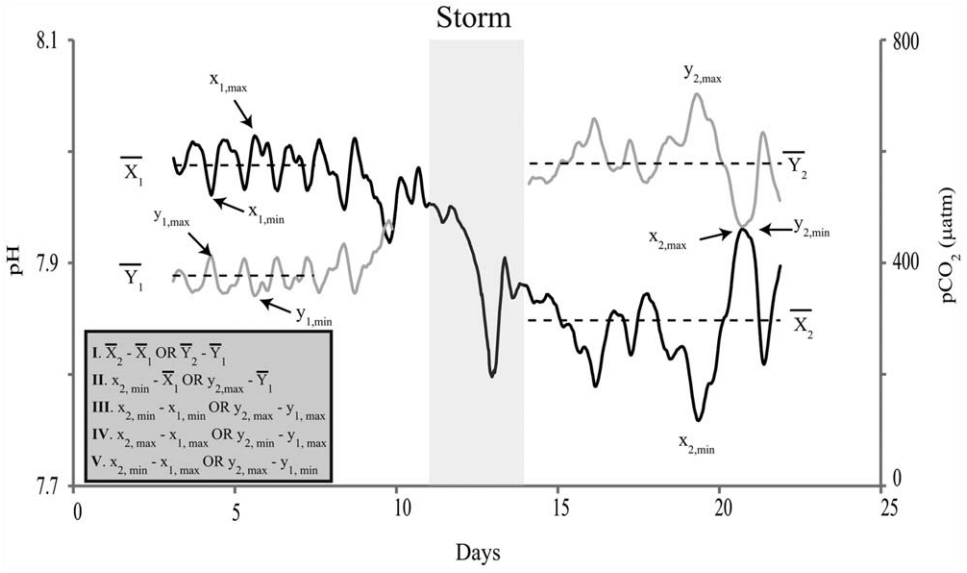

Figure 2. Different aspects of change to carbonate system due to Tropical Storm Isaac**.** Data smoothed for clarity.

poststorm, we used a constant salinity of 36 psu for all calculations of carbonate saturation state after the storm. In situ temperature was collected on the SeaFET pH sensors and inputted into the CO_2-system calculations.

[6] With this in mind, we examined how declines in salinity of 2 and 4 psu would affect our poststorm calculation of Ω_{arag}. If salinity was 34 and 32 psu, rather than the inputted 36, mean Ω_{arag} (Min – Max) would have been 2.38 (1.85 – 3.03) and 2.28 (1.77 – 2.9), respectively. As a result, we consider the results we present for Ω_{arag} to be conservative estimates of post-Isaac saturation state because if salinity was lower than 36 (as it likely was), the change in Ω_{arag} would have been greater than what we report.

2.2. Change in Carbonate Chemistry From Storm Impacts

[7] We present five metrics to best represent changes in carbonate chemistry as caused by the storm. First, we determined the average change of conditions due to the storm, calculated by subtracting the poststorm mean from the prestorm mean (equation (1), Figure 2). The second change of relevance is the most extreme value experienced after the storm (minimum for pH, maximum for $pCO_{2,sw}$) minus the prestorm mean (equation (2), Figure 2). This is the maximum deviation from the prestorm average. Third, is the change in minimum pH, and maximum $pCO_{2,sw}$ values experienced before and after the storm (equation (3), Figure 2). Fourth is the difference between the post and prestorm peaks in pH and minimums in $pCO_{2,sw}$ (equation (4), Figure 2). Lastly is the greatest amplitude of change, which for pH is the difference between the poststorm minimum value and prestorm maximum (equation (5), Figure 2). For $pCO_{2,sw}$, this is the poststorm maximum minus the prestorm minimum. Ω values followed the same trends as pH. We consider the average (equation (1)) and maximum deviations (equation (2)) from the prestorm mean conditions as the most relevant metrics of change due to storm passage. The changes in the minimum and maximum values are informative because they illustrate how diel amplitude is altered by the storm. For ΔΩ, the depression of minimum and maximum Ω (equations (3) and (4)) was roughly equal to the overall mean decline (equation (1), Table 1).

2.3. Modeling Storm Impacts With Ocean Acidification and Warming

[8] To model how ocean acidification will affect the response of coral reef seawater to tropical cyclones, we used the mean conditions previously reported during autumn from nearshore in the middle Florida Keys [*Manzello et al*., 2012]. These data were obtained via bottle samples and dissolved inorganic carbon (DIC) and total alkalinity (TA) were measured directly, yielding mean values of TA = 2388.0 µeq kg^{-1}, DIC = 2078.8 mmol kg^{-1}, $pCO_{2,sw}$ = 404 µatm, Ω_{arag} = 3.47, S = 35.928 practical salinity units (psu), and T = 23.77°C. This $pCO_{2,sw}$ and TA were used as the prestorm mean conditions because this is where Cheeca Rocks is located, conditions were similar to prestorm mean conditions at Cheeca Rocks prior to TS Isaac (prestorm mean $pCO_{2,sw}$ = 382 µatm, Ω_{arag} = 3.48), and most importantly, the TA calculated from the paired pH and $pCO_{2,sw}$ values are unreliable [*Gray et al*., 2011]. Indeed, the mean TA values calculated for the poststorm mean paired pH and $pCO_{2,sw}$ were very low at 2008.5 µeq kg^{-1}. The change in Ω_{arag} reported is reasonable because these same authors showed that paired pH and $pCO_{2,sw}$ values accurately predict Ω_{arag}. Use of these autumn values are valid because the Ω_{arag} values for the prestorm conditions used here are nearly identical to the autumn values in Puerto Rico [*Gray et al*., 2012], thus the model output is applicable to the wider Caribbean. We applied the mean and max post-Isaac changes in $pCO_{2,sw}$ (+196 and + 320 µatm, respectively) to the mean autumn conditions to estimate the response of a tropical storm. By assuming

Table 1. Magnitude of Change in CO_2 Parameters Due to TS Isaac[a]

Cheeca Rocks	ΔpH_T	$\Delta\Omega_{arag}$	$\Delta\Omega_{Mg\text{-}calcite\ (15\ mol\ \%)}$	$\Delta\Omega_{Mg\text{-}calcite\ (18\ mol\ \%)}$	ΔpCO_2 (µatm)	Equation
Poststorm Mean – prestorm Mean	**−0.151**	**−1.00**	**−0.99**	**−0.93**	**+196**	**1**
Poststorm Min – prestorm Mean	**−0.243**	**−1.55**	**−1.53**	**−1.45**	**+320** (Max – Mean)	**2**
Poststorm Max – prestorm Mean	−0.057	−0.34	−0.33	−0.31	+62 (Min – Mean)	
Poststorm Mean – prestorm Min	−0.113	−0.44	−0.44	−0.41	+146 (Mean – Max)	
Poststorm Min – prestorm Min	**−0.205**	**−0.99**	**−0.98**	**−0.93**	**+270** (Max – Max)	**3**
Poststorm Max – prestorm Min	−0.019	+0.22	+0.22	+0.21	+12 (Min – Max)	
Poststorm Mean – prestorm Max	−0.184	−1.70	−1.70	−1.59	+230 (Mean – Min)	
Poststorm Max – prestorm Max	**−0.090**	**−1.04**	**−1.04**	**−0.97**	**+96** (Min – Min)	**4**
Poststorm Min – prestorm Max	**−0.276**	**−2.25**	**−2.24**	**−2.11**	**+354** (Max – Min)	**5**
Little Conch						
Poststorm Mean – prestorm Mean	**−0.177**	N/A	N/A	N/A	N/A	**1**
Poststorm Min – prestorm Mean	**−0.248**	N/A	N/A	N/A	N/A	**2**
Poststorm Max – prestorm Mean	−0.083	N/A	N/A	N/A	N/A	
Poststorm Mean – prestorm Min	−0.132	N/A	N/A	N/A	N/A	
Poststorm Min – prestorm Min	**−0.203**	N/A	N/A	N/A	N/A	**3**
Poststorm Max – prestorm Min	−0.038	N/A	N/A	N/A	N/A	
Poststorm Mean – prestorm Max	−0.250	N/A	N/A	N/A	N/A	
Poststorm Max – Prestorm Max	**−0.156**	N/A	N/A	N/A	N/A	**4**
Poststorm Min – Prestorm Max	**−0.321**	N/A	N/A	N/A	N/A	**5**

[a]Max values in pH and Ω_{arag} correspond to minimum values in pCO_2 as indicated by parenthesis after ΔpCO_2 values. Equations in Figure 2.

constant TA and altering only $pCO_{2,sw}$, we calculated how Ω_{arag} would change with ocean acidification and with +2 and +4°C of warming. An atmospheric $pCO_{2,atm}$ of 390 ppm was used for present-day conditions and values were modeled at increments of 100 µatm assuming +100 ppm $pCO_{2,atm}$ equals approximately +100 µatm $pCO_{2,sw}$.

2.4. Effects of Storm Water Runoff on Carbonate Chemistry

[9] The impact of freshening from storm water runoff is poorly understood. To examine the changes in carbonate chemistry due to storm water runoff on the FRT, new and previously published data collected from September 2009 to October 2012 were analyzed ($n = 64$ bottle samples analyzed for DIC and TA, see *Manzello et al*. [2012] for methods on collection/analysis). Only samples collected in the upper and middle Florida Keys when sea temperatures >25°C were used, as these are most pertinent to when tropical storms are a factor for this region. To understand the impacts of storm runoff on DIC and TA, we examined samples with salinity ≤36 collected after known periods of high rainfall. DIC and TA were first salinity normalized ($nDIC = DIC * 35/S$) and then regressed against salinity. A significant regression was found for both nDIC ($R^2 = 0.84$, $nDIC = -65.381 * S + 4311.5$) and nTA ($R^2 = 0.72$, $nTA = -48.269 * S + 4043.2$) (Figure 3). The relationship of nDIC and nTA with salinity (i.e., slope) was then applied to the post-Isaac values of nDIC and nTA (calculated from TA and $pCO_{2,sw}$) to estimate how they would change from a coincident depression in salinity of −2 and −4 due to runoff. These salinity declines are well within the range for what occurs from a tropical cyclone [*Goreau*, 1964; *Nadaoka et al*., 2001; *Gray et al*., 2012]. With these values of nDIC and nTA, we calculated $pCO_{2,sw}$ and Ω values that would have been observed if a storm-induced salinity drop from runoff of −2 and −4 also occurred. Different ocean acidification scenarios were modeled based on pCO_2 and nTA, assuming constant nTA.

2.5. Calculation of High-Mg Calcite Saturation State

[10] High-Mg calcite mineral phases can be abundant on coral reefs and more soluble than aragonite. In general, a higher mol % of magnesium leads to increased solubility, although there are notable exceptions to this trend [*Kline et al*., 2012; *Nash et al*., 2013]. Stoichiometric solubility

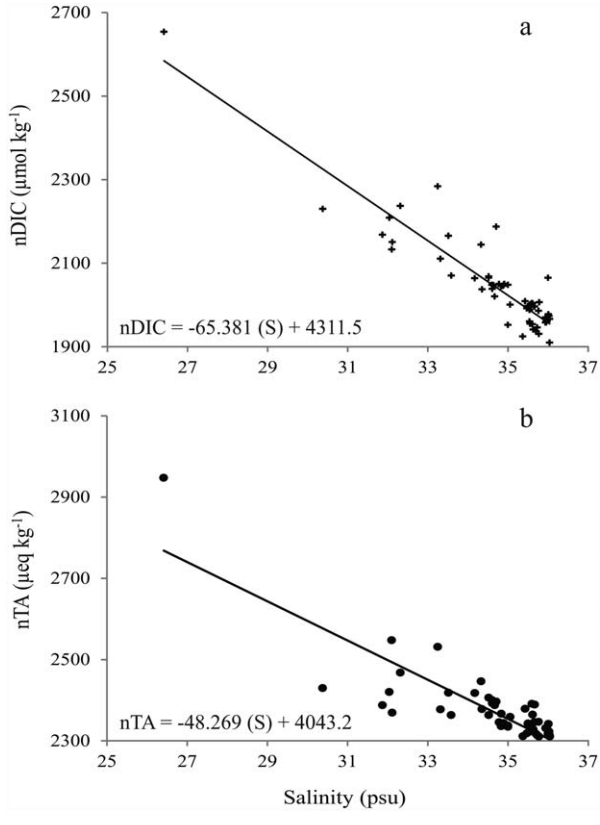

Figure 3. Regression of (a) nDIC and (b) nTA with salinity. Regression equations shown on plot.

Table 2. Values of pH, pCO_2, Ω_{arag}, $\Omega_{Mg\text{-}calcite\ (15\ mol\ \%)}$, and $\Omega_{Mg\text{-}calcite\ (18\ mol\ \%)}$ Before and After Tropical Storm Isaac at Cheeca Rocks and Little Conch Reef

	pH_T	pCO_2 (μatm)	Ω_{arag}	$\Omega_{Mg\text{-}calcite\ (15\ mol\ \%)}$	$\Omega_{Mg\text{-}calcite\ (18\ mol\ \%)}$
	Mean (Min – Max)	Mean (Min – Max)	Mean (Min – Max)	Mean (Min – Max)	Mean (Min – Max)
Before the Storm					
Cheeca Rocks	8.005 (7.967 – 8.038)	382 (348 – 432)	3.48 (2.92 – 4.18)	3.44 (2.89 – 4.15)	3.24 (2.72 – 3.90)
Little Conch	8.024 (7.979 – 8.097)	N/A	N/A	N/A	N/A
After the Storm					
Cheeca Rocks	7.854 (7.762 – 7.948)	578 (444 – 702)	2.48 (1.93 – 3.14)	2.45 (1.91 – 3.11)	2.31 (1.79 – 2.93)
Little Conch	7.847 (7.776 – 7.941)	N/A	N/A	N/A	N/A

products (K'_{sp}) have not been determined for Mg-calcite minerals [*Andersson et al*., 2008]. As a result, the saturation state for mg-calcite mineral phases has to be estimated based on ion activities. We used the relationship for Ion Activity Product (IAP) based on mole fraction of the "best-fit" biogenic high-Mg calcite for cleaned/annealed materials presented in *Morse et al*. [2006] to calculate $\Omega_{Mg\text{-}calcite}$ at 15 and 18 mol %, which are conservative estimates of solubility. The initial estimates based on untreated materials by *Plummer and Mackenzie* [1974] produced solubilities for Mg-calcites that were five times greater than that of aragonite. In fact, if we use the solubilities of *Plummer and Mackenzie* [1974], both 15 and 18 mol % mg-calcite were already undersaturated ($\Omega_{Mg\text{-}calcite} < 1.0$) at the prestorm conditions where mean $\Omega_{arag} = 3.48$ (Table 2).

3. Results and Discussion

3.1. Response of Coral Reef Seawater CO_2 to Tropical Storm Isaac

[11] Tropical Storm Isaac caused both an immediate and prolonged decline in seawater pH on the two coral reefs studied herein (Figure 4). The lowest pH values during the storm occurred in the early evening on 25 August for Little Conch Reef ($pH_T = 7.815$), and on 26 August for Cheeca Rocks ($pH_T = 7.780$) (Figure 4). This represented a decline in pH (relative to prestorm mean) of 0.225 and 0.209 at Cheeca Rocks and Little Conch Reef, respectively (Table 2). Maximum hourly averaged wind speeds and gusts at nearby Molasses Reef were 19.9 and 25.9 m s^{-1}, respectively (Figure 4c). The minimum sea temperatures were 3.49 and 3.19°C lower than the prestorm mean value at Cheeca Rocks and Little Conch Reef, respectively, coincident with the passage of Isaac (Figure 4 and Table 3). There was no measureable photosynthetically active radiation (PAR) at both reef sites for 2 days during the storm (26 and 27 August) and values were very low on 24 and 25 August (Figure 4b).

[12] Following the passage of TS Isaac, winds declined, while temperatures and PAR increased at both sites. However, pH values, after initially increasing following the direct storm-induced minimum, declined at both sites and reached a second minimum value lower than that observed during the storm. This second minimum pH value occurred exactly 1 week later than the first at both sites with pH values of 7.762 and 7.776 at Cheeca Rocks and Little Conch, respectively ($\Delta pH = -0.243$ and -0.248 from prestorm mean, Table 1). When minimum pH values were reached at Cheeca Rocks, the partial pressure of CO_2 in seawater ($pCO_{2,sw}$) reached its maximum poststorm value of 702 μatm (Table 2). The maximum poststorm $pCO_{2,sw}$ value was 320 μatm greater, while the mean poststorm $pCO_{2,sw}$ value was 196 μatm greater than prestorm average conditions (Table 1). The std. error (SEM) in mean post-Isaac pH and pCO_2 at Cheeca Rocks was nearly double the prestorm values, with SEM values for pH increasing to 0.0021 from 0.0011 and pCO_2 from 3.1 to 7.5. The variance in pH at Little Conch increased as well after the storm, but less so from 0.0016 to 0.0018. The mean (± std. error) change in

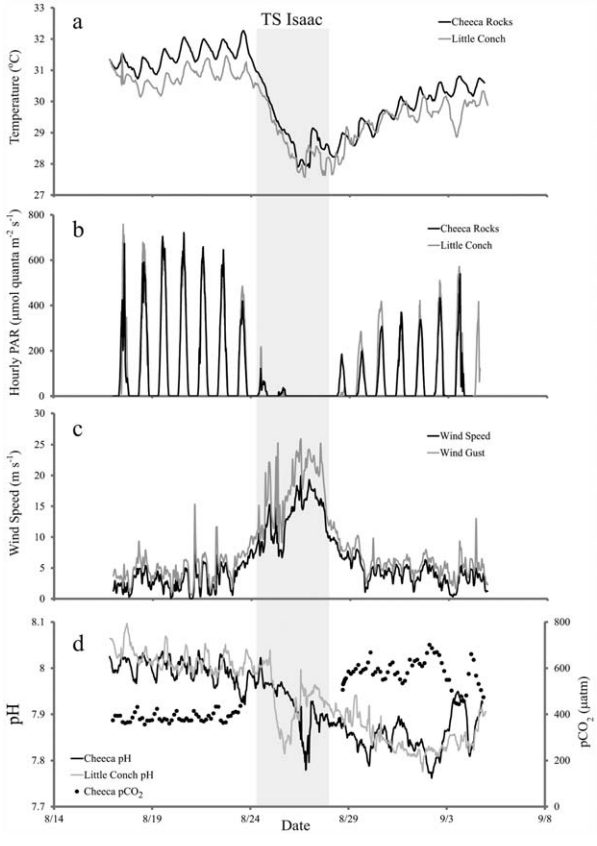

Figure 4. Oceanographic and meteorological conditions during passage of Tropical Storm Isaac. (a) Seawater temperature in °C. (b) Hourly average Photosynthetically Active Radiation (PAR). (c) Wind speeds and gusts at Molasses Reef. (d) pH and pCO_2 (Cheeca Rocks only).

Table 3. Seawater Temperature (°C) Before, During, and After Tropical Storm Isaac[a]

	Before the Storm		During the Storm				After the Storm	
Site	Mean	Min – Max	Min	$\Delta_{Max-Min}$	$\Delta_{Mean-Min}$	$\Delta_{Min-Min}$	Mean	Min – Max
Cheeca Rocks	31.37	30.73 – 32.27	27.88	4.39	3.49	2.85	29.89	28.58 – 30.81
Little Conch	30.77	30.14 – 31.56	27.58	3.89	3.19	2.56	29.55	28.58 – 30.34

[a] $\Delta_{Max-Min}$, $\Delta_{Mean-Min}$, and $\Delta_{Min-Min}$ denote the difference between prestorm value (Max, Mean, and Min) and the Min value during the storm.

aragonite saturation state (Ω_{arag}) was −1.0 (±0.039), for a full week after the storm impact, with a minimum post-storm Ω_{arag} value of 1.93, which was 1.55 less than the prestorm mean (Tables 1 and 2).

3.2. Response of Coral Reef Seawater CO_2 to Storms and Seawater Freshening in a High-CO_2 World

[13] Figure 5 shows the mean (a, c) and extreme (b, d) response of aragonite (Ω_{arag}) and high-Mg calcite saturation ($\Omega_{Mg\text{-}calcite\ (18\ mol\ \%)}$) to tropical storm impacts with coincident freshening from runoff and warming as a function of $pCO_{2,atm}$. The mean response represents the 7 day mean response that occurred after TS Isaac, thus these conditions are the mean conditions expected for a full week in duration after at storm. The response of $\Omega_{Mg\text{-}calcite\ (15\ mol\ \%)}$ is not shown because values are similar to Ω_{arag} (see Tables 4 and 5). Figure 6 shows the response of $pCO_{2,sw}$. If salinity declines by 2 and 4 from storm water runoff, the decline in Ω increases by 0.27 and 0.47 for aragonite and 0.25 and 0.43 for 18 mol % mg-calcite, respectively. For conditions expected by the end of this century ($pCO_{2,atm} = 935$ ppm), mean Ω_{arag}, $\Omega_{Mg\text{-}calcite\ (15\ mol\ \%)}$, and $\Omega_{Mg\text{-}calcite\ (18\ mol\ \%)} = 1.53$, 1.51, and 1.42 from storm impacts without any runoff (Table 4 and Figure 5). With a runoff-induced salinity change of −2, Ω_{arag}, $\Omega_{Mg\text{-}calcite\ (15\ mol\ \%)}$, and $\Omega_{Mg\text{-}calcite\ (18\ mol\ \%)} = 1.26$, 1.25, and 1.17. For a change in salinity of −4, the mean value for 18 mol % is undersaturated ($\Omega < 1.0$), while Ω_{arag} and $\Omega_{Mg\text{-}calcite\ (15\ mol\ \%)}$ are slightly above thermodynamic equilibrium (Table 4). Minimum Ω values are all undersaturated by the end of the century when salinity is reduced by −4 psu due to runoff from storm impacts (Table 4). The magnitude of these changes decreases only slightly with +2

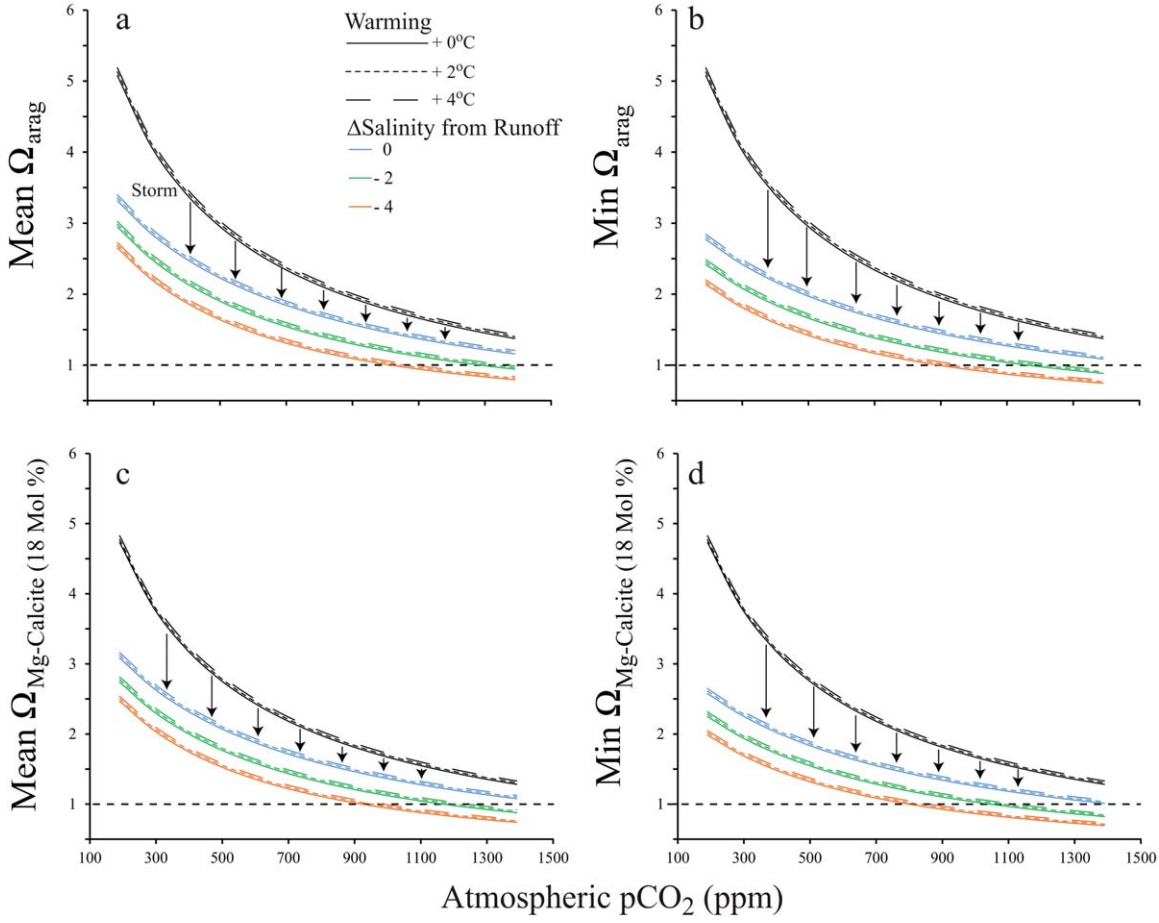

Figure 5. (a and b) Mean and Minimum Ω_{arag} and (c and d) $\Omega_{Mg\text{-}calcite\ (18\ mol\ \%)}$ due to tropical storm impacts at salinity reductions due to freshening from runoff of 0, −2, and −4 with +0, +2, and +4°C of warming as a function of atmospheric pCO_2 (ppm). Nondashed black line is prestorm mean conditions.

Table 4. Aragonite (Ω_{arag}) and High-Mg Calcite ($\Omega_{Mg\text{-}Calcite}$) Saturation State at Atmospheric pCO_2 of 935 ppm for Change in Salinity (ΔS) Due to Storm Water Runoff of −0, −2, and −4 and Warming of +0, +2, and +4°C

	Mean Ω_{arag}			Min Ω_{arag}		
ΔS	+0°C	+2°C	+4°C	+0°C	+2°C	+4°C
−0	1.53	1.56	1.59	1.41	1.43	1.46
−2	1.26	1.29	1.32	1.16	1.18	1.21
−4	1.06	1.09	1.11	0.97	0.99	1.02
	Mean $\Omega_{Mg\text{-}Calcite\ (15\ mol\ \%)}$			Min $\Omega_{Mg\text{-}Calcite\ (15\ mol\ \%)}$		
ΔS	+0°C	+2°C	+4°C	+0°C	+2°C	+4°C
−0	1.51	1.54	1.57	1.40	1.41	1.45
−2	1.25	1.28	1.31	1.15	1.17	1.20
−4	1.05	1.08	1.10	0.96	0.98	1.01
	Mean $\Omega_{Mg\text{-}Calcite\ (18\ mol\ \%)}$			Min $\Omega_{Mg\text{-}Calcite\ (18\ mol\ \%)}$		
ΔS	+0°C	+2°C	+4°C	+0°C	+2°C	+4°C
−0	1.42	1.45	1.48	1.31	1.33	1.36
−2	1.17	1.20	1.23	1.08	1.10	1.13
−4	0.99	1.01	1.03	0.90	0.92	0.95

and +4°C of warming. Near the end of this century, week-long periods of high-Mg calcite (18 mol %) undersaturation can occur as a result of tropical cyclones with high rainfall.

[14] Periods of aragonite undersaturation will begin to occur at atmospheric $pCO_{2,atm}$ levels of 902, 1172, and 1574 ppm when salinities are depressed by −4, −2, and 0 from runoff (Table 5). The projected occurrences of undersaturation of 15 mol % mg-calcite are similar to aragonite, but occur at slightly lower levels of atmospheric $pCO_{2,atm}$ (Table 5). Periods of undersaturation with respect to 18 mol % mg-calcite begin to occur at $pCO_{2,atm}$ of 805, 1052, and 1335 ppm for poststorm salinity depressions of −4, −2, and 0 from runoff. Values of $pCO_{2,atm}$ of 805–902 ppm are expected to occur before the end of this century based on the "business-as-usual" scenario (RCP 8.5 projections) [*Riahi et al*., 2007]. Warming of +2 and +4°C only increases the $pCO_{2,atm}$ required to elicit $\Omega < 1.0$ by 27–34 and 63–71 ppm, respectively.

[15] Freshening of seawater alters the carbonate chemistry differently depending on the concentration of DIC and TA of the freshwater input. Riverine inputs are often acidic, but if the catchment is limestone rich, or influenced by agricultural liming, this acidity can be buffered [*Kawahata et al*., 2000; *Salisbury et al*., 2008; *Tyrrell et al*., 2008]. Groundwater freshening lowers pH and Ω_{arag}, while elevating $pCO_{2,sw}$ [*Kawahata et al*., 2000; *Crook et al*., 2012]. Freshwater inputs from the Florida Everglades, which behaves as a slow moving river with a limestone catchment, have high TA, but also very high DIC from remineralization of organic material that elevates $pCO_{2,sw}$ and depresses Ω_{arag} [*Millero et al*., 2001]. Our data show that freshening from runoff in the Florida Keys causes elevated $pCO_{2,sw}$ and depressed Ω_{arag}.

[16] Shallow-water coral reef flats and lagoons have large diel ranges in carbonate chemistry that can exceed the

Table 5. Atmospheric pCO_2 (ppm) Value Where Aragonite and High-Mg Calcite (15 and 18 mol %) is in Thermodynamic Equilibrium ($\Omega = 1.0$) and Undersaturated ($\Omega < 1.0$) for Change in Salinity (ΔS) Due to Storm Water Runoff of −0, −2, and −4 and Warming of +0, +2, and +4°C

	pCO_2 When Mean $\Omega_{arag} = 1.0$			pCO_2 When Min $\Omega_{arag} = 1.0$		
ΔS	+0°C	+2°C	+4°C	+0°C	+2°C	+4°C
−0	1676	1726	1786	1552	1602	1662
−2	1279	1319	1363	1155	1195	1236
−4	1012	1045	1081	888	921	957
	pCO_2 When Mean $\Omega_{arag} < 1.0$			pCO_2 When Min $\Omega_{arag} < 1.0$		
ΔS	+0°C	+2°C	+4°C	+0°C	+2°C	+4°C
−0	1698	1748	1803	1574	1624	1679
−2	1296	1337	1381	1172	1213	1257
−4	1026	1060	1097	902	936	973
	pCO_2 When Mean $\Omega_{Mg\text{-}Calcite\ (15\ mol\ \%)} = 1.0$			pCO_2 When Min $\Omega_{Mg\text{-}Calcite\ (15\ mol\ \%)} = 1.0$		
ΔS	+0°C	+2°C	+4°C	+0°C	+2°C	+4°C
−0	1652	1702	1755	1528	1578	1631
−2	1260	1300	1343	1136	1176	1219
−4	996	1029	1065	872	905	941
	pCO_2 When Mean $\Omega_{Mg\text{-}Calcite\ (15\ mol\ \%)} < 1.0$			pCO_2 When Min $\Omega_{Mg\text{-}Calcite\ (15\ mol\ \%)} < 1.0$		
ΔS	+0°C	+2°C	+4°C	+0°C	+2°C	+4°C
−0	1674	1724	1779	1550	1600	1655
−2	1277	1317	1362	1153	1194	1238
−4	1010	1044	1080	886	920	956
	pCO_2 When Mean $\Omega_{Mg\text{-}Calcite\ (18\ mol\ \%)} = 1.0$			pCO_2 When Min $\Omega_{Mg\text{-}Calcite\ (18\ mol\ \%)} = 1.0$		
ΔS	+0°C	+2°C	+4°C	+0°C	+2°C	+4°C
−0	1525	1570	1619	1315	1360	1409
−2	1160	1196	1234	1036	1072	1110
−4	916	945	978	792	821	854
	pCO_2 When Mean $\Omega_{Mg\text{-}Calcite\ (18\ mol\ \%)} < 1.0$			pCO_2 When Min $\Omega_{Mg\text{-}Calcite\ (18\ mol\ \%)} < 1.0$		
ΔS	+0°C	+2°C	+4°C	+0°C	+2°C	+4°C
−0	1545	1591	1640	1335	1381	1430
−2	1176	1212	1251	1052	1088	1127
−4	929	956	992	805	832	868

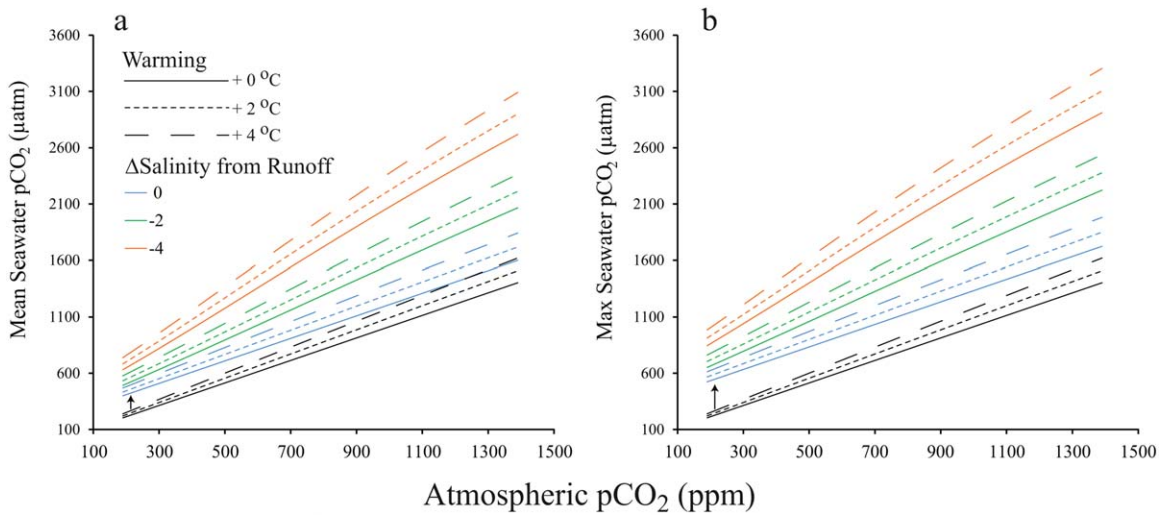

Figure 6. (a) Mean and (b) maximum pCO_2 (µatm) following tropical storm impacts at salinity reductions due to freshening from runoff of 0, −2, and −4 with +0, +2, and +4°C of warming as a function of atmospheric pCO_2 (ppm).

magnitude of change from ocean acidification expected over the next century [*Ohde and van Woesik*, 1999; *Santos et al*., 2011; *Kline et al*., 2012; *Shaw et al*., 2012]. The small water volume of shallow environments causes a magnification of the benthic metabolic signal [e.g., *Manzello*, 2010]. The depths of the two reefs studied here are ∼3–8 m (Little Conch Reef = 5–8 m depth, Cheeca Rocks = 3–7 m, though isolated coral patches come within 1–2 m of the surface). Thus, we anticipate that the storm changes will be greater, and that periods of undersaturation will occur sooner, for shallower reef communities where large diel ranges occur normally.

[17] The existing data illustrate impacts from relatively benign tropical storms (max winds = 12 and ∼20 m s^{-1}). It seems likely that the impacts from hurricanes, tropical cyclones, and typhoons (>33 m s^{-1}) [*Simpson and Riehl*, 1981] would cause greater changes to the seawater CO_2 system. Storm impacts represent short term, stochastic, but increasingly important events in the $CaCO_3$ cycle of coral reefs. We show that as ocean acidification progresses, short-term corrosive events from storm impacts increase in both severity and duration. Although tropical cyclone cooling has been shown to be a viable mechanism to reduce thermal stress to coral reefs [*Manzello et al*., 2007; *Carrigan and Puotinen*, 2011], these data suggest that despite providing thermal respite to living corals, tropical cyclones in combination with ocean acidification can cause $CaCO_3$ undersaturation, potentially undercutting the cooling benefit over time by favoring direct chemical dissolution that may reduce viable habitat.

[18] The estimates presented herein predicting abiotic $CaCO_3$ dissolution with storm impacts and ocean acidification are conservative. In reality, $CaCO_3$ dissolution occurs at Ω_{arag} values far greater than undersaturation [e.g., *Kline et al*., 2012]. Recent experimental work has shown that dissolution occurs at $\Omega_{arag} > 3.0$ for reef sediments and high-Mg calcite crustose coralline algae (CCA) [*Yamamoto et al*., 2012; *Kline et al*., 2012]. Dissolution rates are not always a direct function of [Mg], however, as some CCA have been recently shown to possess dolomite, which is less soluble than aragonite [*Nash et al*., 2013]. Regardless, dissolution is already occurring on coral reefs and will increase with acidification. The ocean acidification levels when reefs experience net dissolution is debatable, but estimates have been proposed that this will occur globally with a doubling of atmospheric CO_2 [*Silverman et al*., 2009], or even as low as $pCO_{2,sw}$ values of 467 µatm for certain reef substrates [*Yates and Halley*, 2006].

3.3. Factors Causing Changes in Seawater CO_2 Due to Storms

[19] The response of the coral reef seawater CO_2 system to tropical storm passage is complex and dependent on a number of factors, such as storm intensity, distance from center of the storm, and rainfall associated with the storm. Based on our data and the sole previous study [*Gray et al*., 2012], we now know that coral reef Ω_{arag} values are greatly depressed by tropical cyclones. The impairment and/or cessation of photosynthesis, inferred from the lack of PAR for 2 days during the storm, would by itself cause a decline in pH and elevation in $pCO_{2,sw}$ due to alteration of the photosynthesis/respiration (P/R) ratio of the benthic community. A decline in PAR associated with a tropical storm did indeed cause a decrease in diel variability of pH, $pCO_{2,sw}$, and O_2 on a Puerto Rican reef [*Gray et al*., 2012]. In addition to a reduction in photosynthesis, respiration may increase as a result of the hydrodynamic disturbance, sedimentation, and depressed salinity associated with storm activity [*Nystrom et al*., 1997]. Windy conditions are associated with sediment resuspension and substantial alteration of sediment topology was observed by divers at study sites following TS Isaac. Sediment pore-waters are known to be more acidic and exhibit higher $pCO_{2,sw}$ relative to the overlying water column due to remineralization of organic matter [*Tribble*, 1993], thus sediment resuspension mixes corrosive pore-waters into the water column. During normal conditions, $CaCO_3$ sediments exhibit net dissolution (net TA flux out of the sediments) [*Rao et al*., 2012; *Cyronak et al*., 2013]. This dissolution is due to the respiratory buildup of metabolic CO_2 in the pore-waters,

which is stimulated by advection of the overlying water into the sediments and PAR [*Cyronak et al*., 2013]. The turbulent mixing of the water column and sediments during a tropical storm would cause substantial disturbance and it is not completely clear how the metabolism measured under quiescent conditions would apply. Dissolution is directly linked to both PAR and the buildup of respiratory CO_2, thus the strong mixing and likely oxygenation of the sediments, as well as the depressed PAR during storms would be expected to impair this normal dissolution. This reduction of TA flux from the sediments would act to further elevate pCO_2 and lower Ω_{arag}. Elevated $pCO_{2,sw}$ did occur coincident with prior windy and cloudy conditions on the FRT [*Manzello et al*., 2012], showing that decreases in PAR and/or sediment resuspension correlate with and may cause declines in pH. Lastly, upwelling due to storms brings deeper, CO_2-enriched waters to the surface layers [*Nemoto et al*., 2009; *Bond et al*., 2011].

[20] The data presented here show that there was a lingering community metabolic distress that occurred after TS Isaac, as indicated by the second minimum in pH at both reef sites a full week following the storm impact (Figure 4d). The increase in variance of the pH and $pCO_{2,sw}$ data after TS Isaac suggests that there was community metabolic disturbance. In fact, pH values continued along a downward trajectory after initially increasing immediately after the storm. Similarly, *Gray et al*. [2012] observed a period of net respiration after a tropical storm, causing the aforementioned lowest recorded pH (7.89) and Ω_{arag} ($\leq$3) of their 2 year investigation. The diurnal cycle in pH is linked to photosynthesis-induced maximum values during the day and respiratory-induced minimum values at night [*Kayanne et al*., 1995; *Kleypas et al*., 2011; *Gray et al*., 2012] (Figures 4b and 4d). Only when PAR values reached levels similar to what occurred prior to TS Isaac did the pH trajectory start to reverse. The responses at both sites were remarkably similar, which suggests that mechanisms causing these changes were occurring at a regional, rather than a local scale.

[21] *Drupp et al*. [2011] and *Gray et al*. [2012] observed algal blooms in the water column following storms that were associated with an increase in pH and decline in $pCO_{2,sw}$. The algal bloom and $pCO_{2,sw}$ decline in Puerto Rico was short lived and followed thereafter by depressed pH. This initial decrease in $pCO_{2,sw}$ and corresponding increase in pH and Ω_{arag} was not observed in Florida, as pH was chronically depressed after the storm (Figure 4). We hypothesize that the stress on the benthic community was greater in our study, such that any water column increase in productivity was indiscernible relative to the benthic stress signal. The responses in Hawaii corresponded to storm events that were not tropical storms and TS Isaac more severely impacted the FRT compared to the Puerto Rican study. PAR was always measureable in Puerto Rico and max hourly wind speeds peaked at 12 m s^{-1} versus 19.9 m s^{-1} from TS Isaac [*Gray et al*., 2012].

4. Conclusions

[22] Coral reefs are in decline globally and the situation is particularly concerning in the Caribbean. For Caribbean reefs, live coral cover has declined by about 80% since the 1970s, $CaCO_3$ production is down to 50% below historical averages, and more than a third of sites recently surveyed (37%) were already net erosional [*Gardner et al*., 2003; *Perry et al*., 2013]. Many Caribbean reefs are, or are close to $CaCO_3$ budget neutral, termed "accretionary stasis," suggesting that the continued persistence of architecturally complex reef framework structures is questionable [*Perry et al*., 2013].

[23] In conclusion, the existence of coral reefs beyond this century is in jeopardy. The concern has gone from the drastic declines in living coral cover [*Gardner et al*., 2003], to fear that the very framework of coral reefs will erode away [*Hoegh-Guldberg et al*., 2007; *Manzello et al*., 2008; *Perry et al*., 2013]. All concerns regarding ocean acidification assumed that aragonite undersaturation would not occur on coral reefs within the foreseeable future due to their location within the highly supersaturated tropical oceans [*Kleypas et al*., 1999]. We show, for the first time, that $CaCO_3$ undersaturation will occur in a high-CO_2 world as a result of modest tropical cyclones. Approximately 81 hurricanes made landfall in south Florida over the period 1851–2005, which is a frequency of roughly one hurricane impact every 2 years [*Manzello et al*., 2007]. The duration of corrosive waters may be short (days to weeks), but the importance of these events becomes more apparent when the routine nature of tropical storms is considered over longer time scales (centuries to millennia). The expected increase in the strength, frequency, and rainfall of the most severe tropical cyclones in combination with ocean acidification will have serious consequences for the persistence of coral reef framework structures, which is far more alarming than the loss of living coral.

[24] **Acknowledgments.** We thank the National Oceanic and Atmospheric Administration's (NOAA) Coral Reef Conservation Program and Ocean Acidification Program for funding this research. W. McGillis provided salinity data and J. S. Fajans assisted with field work. D. Graham assisted with seawater CO_2 analysis. R. van Hooidonk helped with emission scenarios and A. Sutton provided background information on the effects of tropical cyclones on seawater carbonate chemistry and the $MApCO_2$.

References

Andersson, A. J., F. T. Mackenzie, and N. R. Bates (2008), Life on the margin: Implications of ocean acidification on Mg-calcite, high-latitude and cold-water calcifiers, *Mar. Ecol. Prog. Ser.*, *373*, 265–273, doi:10.3354/meps07639.

Bond, N. A., M. F. Cronin, C. Sabine, Y. Kawai, H. Ichikawa, P. Freitag, and K. Ronnholm (2011), Upper ocean response to Typhoon Choi-Wan as measured by the Kuroshio Extension Observatory mooring, *J. Geophys. Res.*, *116*, C02031, doi:10.1029/2010JC006548.

Carrigan, A. D., and M. L. Puotinen (2011), Assessing the potential for tropical cyclone induced sea surface cooling to reduce thermal stress on the world's coral reefs, *Geophys. Res. Lett.*, *38*, L23604, doi:10.1029/2011GL049722.

Crook, E. D., D. Potts, M. Rebolledo-Vieyra, L. Hernandez, and A. Paytan (2012), Calcifying coral abundance near low-pH springs: Implications for future ocean acidification, *Coral Reefs*, *31*, 239–245, doi:10.1007/s00338-011-0839-y.

Cyronak, T., I. R. Santos, A. McMahon, and B. D. Eyre (2013), Carbon cycling hysteresis in permeable carbonate sands over a diel cycle: Implications for ocean acidification, *Limnol. Oceanogr.*, *58*, 131–143, doi:10.4391/lo.2013.58.1.0131.

Drupp, P., E. H. De Carlo, F. T. Mackenzie, P. Bienfang, and C. L. Sabine (2011), Nutrient inputs, phytoplankton response, and CO2 variations in a semi-enclosed subtropical embayment, Kaneohe Bay, Hawaii, *Aquat. Geochem.*, *17*, 473–498, doi:10.1007/s10498-010-9115-y.

Fabricius, K. E., C. Langdon, S. Uthicke, C. Humphrey, S. Noonan, G. De'ath, R. Okazaki, N. Muehllehner, M. S. Glas, and J. M. Lough (2011), Losers and winners in coral reefs acclimatized to elevated carbon

dioxide concentrations, *Nat. Clim. Change*, *1*, 165–169, doi:10.1038/nclimate1122.

Frieler, K., M. Meinhausen, A. Golly, M. Mengel, K. Lebek, S. D. Donner, and O. Hoegh-Guldberg (2013), Limiting global warming to 2°C is unlikely to save most coral reefs, *Nat. Clim. Change*, *3*, 165–170, doi:10.1038/NCLIMATE1674.

Gardner, T. A., I. M. Cote, J. A. Gill, A. Grant, and A. R. Watkinson (2003), Long-term region-wide declines in Caribbean corals, *Science*, *301*, 958–960, doi:10.1126/science.1086050.

Goreau, T. F. (1964), Mass expulsion of zooxanthellae from Jamaican reef communities after Hurricane Flora, *Science*, *145*, 383–386, doi:10.1126/science.145.3630.383.

Gray, S. E. C., M. D. DeGrandpre, T. S. Moore, T. R. Martz, G. E. Friederich, and K. S. Johnson (2011), Applications of in situ pH measurements for inorganic carbon calculations, *Mar. Chem.*, *125*, 82–90, doi:10.1016/j.marchem.2011.02.005.

Gray, S. E. C., M. D. DeGrandpre, C. Langdon, and J. Corredor (2012), Short-term and seasonal pH, pCO2 and saturation state variability in a coral-reef ecosystem, *Global Biogeochem. Cycles*, *26*, GB3012, doi:10.1029/2011GB004114.

Hoegh-Guldberg, O., et al. (2007), Coral reefs under rapid climate change and ocean acidification, *Science*, *318*, 1737–1742, doi:10.1126/science.1152509.

Hofmann, G. E., et al. (2011), High-frequency dynamics of ocean pH: A multi-ecosystem comparison, *PLoS ONE*, *6*, e28983, doi:10.1371/journal.pone.0028983.

Kawahata, H., I. Yukino, and A. Suzuki (2000), Terrestrial influence on the Shiraho fringing reef, Ishigaki Island, Japan: High carbon input relative to phosphate, *Coral Reefs*, *19*, 172–178.

Kayanne, H., A. Suzuki, and H. Saito (1995), Diurnal changes in the partial pressure of carbon dioxide in coral reef water, *Science*, *269*, 214–216, doi:10.1126/science.269.5221.214.

Kleypas, J. A., R. W. Buddemeier, D. Archer, J. P. Gattuso, C. Langdon, and B. N. Opdyke (1999), Geochemical consequences of increased atmospheric carbon dioxide on coral reefs, *Science*, *284*, 118–120, doi:10.1126/science.284.5411.118.

Kleypas, J. A., K. R. N. Anthony, and J. P. Gattuso (2011), Coral reefs modify their seawater carbon chemistry—Case study from a barrier reef (Moorea, French Polynesia), *Global Change Biol.*, *17*, 3667–3678, doi:10.1111/j.1365–2486.2011.02530.x.

Kline, D. I., et al. (2012), A short-term in situ CO2 enrichment experiment on Heron Island (GBR), *Sci. Rep.*, *2*, 413, doi:10.1038/srep00413.

Knutson, T. R., J. L. McBride, J. Chan, K. Emanuel, G. Holland, C. Landsea, I. Held, J. P. Kossin, A. K. Srivastava, and M. Sugi (2010), Tropical cyclones and climate change, *Nat. Geosci.*, *3*, 157–163, doi:10.1038/NGEO779.

Langdon, C., T. Takahashi, C. Sweeney, D. Chipman, J. Goddard, F. Marubini, H. Aceves, H. Barnett, and M. J. Atkinson (2000), Effect of calcium carbonate saturation state on the calcification rate of an experimental coral reef, *Global Biogeochem. Cycles*, *14*, 639–654, doi:10.1029/1999GB001195.

Lewis, E., and D. W. R. Wallace (1998), Program Developed for CO_2 System Calculations, edited by ORNL/CDIAC-105, 33 pp., Carbon Dioxide Inf. Anal. Cent., Oak Ridge Natl. Lab., U.S. Dept. of Energy, Oak Ridge, Tenn.

Manzello, D. P. (2009), in *Proceedings of the 11th International Coral Reef Symposium*, Nove SE Univ., Ft. Lauderdale, Fla., vol. 1, pp. 1299–1304.

Manzello, D. P. (2010), Ocean acidification hot spots: Spatiotemporal dynamics of the seawater CO2 system of eastern Pacific coral reefs, *Limnol. Oceanogr.*, *55*, 239–248, doi:10.4319/lo.2010.55.1.0239.

Manzello, D. P., M. Brandt, T. B. Smith, D. Lirman, J. C. Hendee, and R. Nemeth (2007), Hurricanes benefit bleached corals, *Proc. Natl. Acad. Sci. U. S. A.*, *104*, 12,035–12,039, doi:10.1073/pnas.0701194104.

Manzello, D. P., J. A. Kleypas, D. A. Budd, C. M. Eakin, P. W. Glynn, and C. Langdon (2008), Poorly cemented coral reefs of the eastern tropical Pacific: Possible insights into reef development in a high-CO_2 world, *Proc. Natl. Acad. Sci. U. S. A.*, *105*, 10,450–10,455, doi:10.1073/pnas. 0712167105.

Manzello, D. P., I. C. Enochs, N. Melo, D. K. Gledhill, and E. M. Johns (2012), Ocean acidification refugia of the Florida reef tract, *PLoS ONE*, *7*, e41715, doi:10.1371/journal.pone.0041715.

Millero, F. J., W. T. Hiscock, F. Huang, M. Roche, and J. Z. Zhang (2001), Seasonal variation of the carbonate system in Florida Bay, *Bull. Mar. Sci.*, *68*, 101–123.

Morse, J. W., A. J. Andersson, and F. T. Mackenzie (2006), Initital responses of carbonate-rich shelf sediments to rising atmospheric pCO2 and ocean acidification: Role of high Mg-calcites, *Geochim. Cosmochim. Acta*, *70*, 5814–5830, doi:10.1016/j.gca.2006.08.017.

Nadaoka, K., Y. Nihei, R. Kumano, T. Yokobori, T. Omija, and K. Wakaki (2001), A field observation on hydrodynamic and thermal environments of a fringing reef at Ishigaki Island under typhoon and normal atmospheric conditions, *Coral Reefs*, *21*, 387–398, doi:10.1007/s00338-001-0188-3.

Nash, M. C., et al. (2013), Dolomite-rich coralline algae in reefs resist dissolution in acidified conditions, *Nat. Clim. Change*, *3*, 268–272, doi:10.1038/NCLIMATE1760.

Nemoto, K., T. Midorikawa, A. Wada, K. Ogawa, S. Takatini, H. Kimoto, M. Ishii, and H. Y. Inoue (2009), Continuous observations of atmospheric and oceanic CO2 using a moored buoy in the East China Sea: Variations during the passage of typhoons, *Deep Sea Res.*, Part II, 56, 542–553, doi:10.1016/j.dsr2.2008.12.015.

Nystrom, M., F. Moberg, and M. Tedengren (1997), Natural and anthropogenic disturbance on reef corals in the inner Gulf of Thailand: Physiological effects of reduced salinity, copper, and siltation, in *Proceedings of the 8th International Coral Reef Symposium*, Smithsonian Tropical Research Institute, Panama, vol. 2, pp. 1893–1898.

Ohde, S., and R. van Woesik (1999), Carbon dioxide flux and metabolic processes of a coral reef, Okinawa, *Bull. Mar. Sci.*, *65*, 559–576.

Perry, C. T., G. N. Murphy, P. S. Kench, S. G. Smithers, E. N. Edinger, R. S. Steneck, and P. J. Mumby (2013), Caribbean-wide decline in carbonate production threatens coral reef growth, *Nat. Commun.*, *4*, 1402, doi:10.1038/ncomms2409.

Plummer, L. N., and F. T. Mackenzie (1974), Predicting mineral solubility from rate data: Application to the dissolution of Mg-calcites, *Am. J. Sci.*, *274*, 61–83.

Rao, A. M. F., L. Polerecky, D. Ionescu, F. J. R. Meysman, and D. de Beer (2012), The influence of pore-water advection, benthic photosynthesis, and respiration on calcium carbonate dynamics in reef sands, *Limnol. Oceanogr.*, *57*, 809–825, doi:10.4319/lo.2012.57.3.0809.

Riahi, K., A. Grübler, and N. Nakicenovic (2007), Scenarios of long-term socio-economic and environmental development under climate stabilization, *Technol. Forecasting Soc. Change*, *74*, 887–935, doi:10.1016/j.techfore.2006.05.026/.

Salisbury, J., M. Green, C. Hunt, and J. Campbell (2008), Coastal acidification by rivers: A threat to shellfish?, *Eos Trans. AGU*, *89*, 50, doi:10.1029/2008EO500001.

Santos, I. R., R. N. Guld, D. Maher, D. Erler, and B. D. Eyre (2011), Diel coral reef acidification driven by porewater advection in permeable carbonate sands, Heron Island, Great Barrier Reef, *Geophys. Res. Lett.*, *38*, L03604, doi:10.1029/2010GL046053.

Scoffin, T. P. (1993), The geological effects of hurricanes on coral reefs and the interpretation of storm deposits, *Coral Reefs*, *12*, 203–221.

Shaw, E. C., B. I. McNeil, and B. Tilbrook (2012), Impacts of ocean acidification in naturally variable coral reef flat ecosystems, *J. Geophys. Res.*, *117*, C03038, doi:10.1029/2011JC007655.

Silverman, J., B. Lazar, L. Cao, K. Caldeira, and J. Erez (2009), Coral reefs may start dissolving when atmospheric CO2 doubles, *Geophys. Res. Lett.*, *36*, L05606, doi:10.1029/2008GL036282.

Simpson, R. H., and H. Riehl (1981), *The Hurricane and its Impact*, La. State Univ. Press, Baton Rouge.

Tribble, G. W. (1993), Organic matter oxidation and aragonite diagenesis in a coral reef, *J. Sediment. Petrol.*, *63*, 523–527.

Tribollet, A., C. Godinot, M. J. Atkinson, and C. Langdon (2009), Effects of elevated pCO2 on dissolution of coral carbonates by microbial euendoliths, *Global Biogeochem. Cycles*, *23*, GB3008, doi:10.1029/2008GB003286.

Tyrrell, T., B. Schneider, A. Charalampopoulou, and U. Riebesell (2008), Coccolithophores and calcite saturation state in the Baltic and Black Seas, *Biogeosciences*, *5*, 485–494, doi:10.5194/bg-5–485-2008.

Vandemark, D., J. Salisbury, C. W. Hunt, S. M. Shellito, J. D. Irish, W. R. McGillis, C. L. Sabine, and S. M. Maenner (2011), Temporal and spatial dynamics of CO2 air-sea flux in the Gulf of Maine, *J. Geophys. Res.*, *116*, C01012, doi:10.1029/2010JC006408.

Villarini, G., and G. A. Vecchi (2012), Twenty-first-century projections of North Atlantic tropical storms from CMIP5 models, *Nat. Clim. Change*, *2*, 604–607, doi:10.1038/NCLIMATE1530.

Yamamoto, S., H. Kayanne, M. Terai, A. Watanabe, K. Kato, A. Negishi, and K. Nozaki (2012), Threshold of carbonate saturation state determined by CO2 control experiment, *Biogeosciences*, *9*, 1441–1450, doi:10.5194/bg-9–1441-2012.

Yates, K. K., and R. B. Halley (2006), CO32− concentration and pCO2 thresholds for calcification and dissolution on the Molokai reef flat, Hawaii, *Biogeosciences*, *3*, 357–369, doi:10.5194/bg-3–357-2006.